# Influence of Conductor Shields on the $Q$-Factors of a $TE_0$ Dielectric Resonator

YOSHIO KOBAYASHI, MEMBER, IEEE, TAKAYUKI AOKI, AND YUKIMASA KABE

*Abstract* —Two approaches due to the complex frequency and to the perturbation theory are described to compute accurately the $Q$-factors of the circularly-symmetric $TE_0$ modes for dielectric rod resonators placed between two parallel conductor plates and in a conductor cavity. These techniques allow us to estimate separately the $Q$-factors due to radiation, conductor, and dielectric losses from only the computation of resonant frequencies by means of the mode-matching method. Validity of the theories is verified by experiments. The influence of the conductor shields on the $Q$-factors is discussed from the computed results. A possibility of realizing high-$Q$ dielectric resonators is suggested.

## I. Introduction

DIELECTRIC RESONATORS widely used in microwave circuits are placed in conductor shields to prevent radiation loss. For the circularly-symmetric $TE_0$ modes of such shielded dielectric resonators, the analyses of $Q$-factors have been treated by several authors [1]–[6]. As the first approach, following the definition $Q = \omega W/P$, where $\omega$ is the resonant angular frequency, we calculate the energy stored $W$ and the average power dissipated $P$ in a resonator. However, the rigorous theory for these resonators is quite involved because the exact field expressions are very complicated [1]; therefore, simplifying approximations are considered [2], [3]. In another approach, the complex frequency is introduced into characteristic equations to determine the resonant frequencies and the $Q$-factors simultaneously. An example for the computation of $Q$-factors due to radiation loss $Q_{rad}$ by this method has been shown in [4]. In a similar way, a technique of computing one due to conductor loss $Q_c$ and one due to the dielectric loss $Q_d$ has been presented by Maj and Modelski [5]. However, their procedure for the $Q_c$ computation, in which a conductor layer is considered in the conductor wall, appears to be rather complicated. The third approach based on the perturbation of cavity walls has been presented, by Kajfez [6], to compute $Q_c$. This is an excellent method since $Q_c$ can be determined from only the computation of resonant frequencies. Unfortunately, a similar analysis for $Q_d$ has not been treated so far.

In this paper, based on the mode-matching method useful for the accurate computation of resonant frequencies [7], [8], two approaches due to the complex frequency and to the perturbation theory are described to accurately compute the $Q$-factors of the $TE_0$ modes for resonator structures shown in Fig. 1. In the former approach, the proper locations of roots on a complex plane are discussed. In the latter, the extension of Kajfez's method to the $Q_d$ computation is realized by means of the cavity-material perturbation. These techniques allow us to estimate separately the influence of the conductor shields on the $Q_{rad}$, $Q_c$, and $Q_d$ values. Validity of the theories is verified by experiments.

Manuscript received April 5, 1985; revised June 27, 1985.
Y. Kobayashi and Y. Kabe are with the Department of Electrical Engineering, Saitama University, Urawa, Saitama 338, Japan.
T. Aoki is with the Transmission Division, NEC Corporation, Kawasaki 211, Japan.

## II. Analysis

### A. Analysis by Complex Frequency Technique

Consider three types of shielded dielectric rod resonators shown in Fig. 1. A dielectric rod of relative permittivity $\epsilon_r$, relative permeability $\mu_r = 1$, and diameter $D$ is placed between two parallel conductor plates as in Fig. 1(a) or (b), or in the center of a conductor cavity of diameter $d$ and length $2h$ as in Fig. 1(c). They are called parallel-plates-image, parallel-plates-open, and cavity-open types, respectively. The conductor and dielectric are supposed to be lossless first.

The $TE_0$ modes for the structure in Fig. 1(b) are analyzed by means of the mode-matching method. From the structural symmetry, the resonant modes can be classified into ones for which the $T$-plane ($r\theta$-plane at $z = 0$) is an electric wall and the others for which it is a magnetic wall. The electric $T$-plane modes also correspond to the one for the structure in Fig. 1(a). The resonator is divided into homogeneous subregions I, II, and III. The electromagnetic fields in each subregion are expanded in eigenmodes which satisfy the boundary conditions on the conductor surface and the $T$-plane. Then, imposing the boundary condition at the interfaces of the subregions and applying the orthogonality of the eigenmodes, we get the homogeneous equations for the expansion coefficients. The resonant frequencies are determined by the condition that the determinant of the coefficient matrix vanishes [7]; that is,

$$\det H = 0 \tag{1}$$

where the matrix element $h_{qp}$ $(q, p = 1, 2, \cdots, N)$ is given

0018-9480/85/1200-1361$01.00 ©1985 IEEE

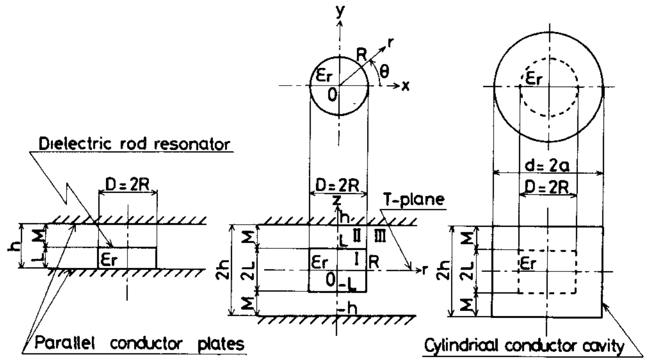


(a) (b) (c)

Fig. 1. Configurations of shielded dielectric rod resonators of three types, i.e., (a) parallel-plates-image type, (b) parallel-plates-open type, and (c) cavity-open type.

by

$$h_{qp} = \frac{\left[\dfrac{J_1(u_p)}{u_p J_0(u_p)} - \dfrac{H_1(v_q)}{v_q H_0(v_q)}\right]\cdot F_{qp}}{\left[X_p^2 - Z_q^2\right]\left[(Y_p/M)^2 - (Z_q/L)^2\right]} \tag{2}$$

$$F_{qp} = \{X_p \cot X_p - Z_q \cot Z_q,\ X_p \tan X_p - Z_q \tan Z_q\} \tag{3}$$

$$u_p = \sqrt{\left(\frac{\omega R}{c}\right)^2 \epsilon_r - \left(\frac{R}{L} X_p\right)^2} \tag{4}$$

$$v_q = \pm\sqrt{\left(\frac{\omega R}{c}\right)^2 - \left(\frac{R}{L} Z_q\right)^2} \tag{5}$$

$$Z_q = \left\{q\pi \frac{L}{h},\ (2q-1)\pi \frac{L}{2h}\right\}. \tag{6}$$

In the above, the first and second expressions in { } correspond to the electric and magnetic $T$-plane modes, respectively. A time factor $e^{j\omega t}$ is tacitly assumed. Also, $c$ is the light velocity in a vacuum, $J_n(x)$ is the Bessel function of the first kind, and $H_n(x)$ is the Hankel function of the second kind. For $u_p$ in (4), a plus sign of the square root is chosen since the term consisting of $J_n(u_p)$ in (2) is an even function for $u_p$, while the choice of the plus or minus signs for $v_p$ in (5) will be discussed later. Furthermore, $(X_p, Y_p)$ is given as the $p$th solution of the following simultaneous equations:

$$\{-X \cot X,\ X \tan X\} = \frac{L}{M} Y \cot Y$$

$$\left(\frac{X}{L}\right)^2 - \left(\frac{Y}{M}\right)^2 = \left(\frac{\omega}{c}\right)^2 (\epsilon_r - 1). \tag{7}$$

To compute the $Q_d$ and $Q_{\text{rad}}$ values as well as the resonant frequencies, we introduce the complex angular frequency

$$\dot{\omega} = \omega_1 + j\omega_2 \quad f_1 = \omega_1/2\pi \quad Q_f = \omega_1/2\omega_2 \tag{8}$$

and the complex relative permittivity

$$\dot{\epsilon}_r = \epsilon_r(1 - j\tan\delta) \tag{9}$$

into (1), where $f_1$ and $Q_f$ are the resonant frequency and $Q$-factor for a damped-free oscillation, respectively, and $\tan\delta$ is the loss tangent of the dielectric. Then, putting $\dot{v}_q = v_{q1} + jv_{q2}$, we get

$$(\omega_1\omega_2/c^2) - (v_{q1}v_{q2}/R^2) = 0 \tag{10}$$

from the imaginary part of $v_q^2$ in (5). Since $\omega_1$ and $\omega_2$ are both positive, $v_{q1}$ and $v_{q2}$ are both positive or both negative, as seen from (10); that is, the roots $\dot{v}_q$ exist in either the first or third quadrant of a complex $v$ plane. Furthermore, the fields outside the rod behave as

$$e^{j(\dot{\omega}t - \dot{v}_q\bar{r})} = e^{-\omega_2 t} e^{v_{q2}\bar{r}} e^{j(\omega_1 t - v_{q1}\bar{r})}, \qquad \bar{r} = \frac{r}{R} \tag{11}$$

since $H_n(x) \simeq (2/\pi x)^{1/2}\exp(-jx + j(2n+1)\pi/4)$ for $1 \ll x\ (= \dot{v}_q\bar{r})$. Some considerations of (11) result in the following: the first quadrant corresponds to a leaky region, where the fields propagate in the positive $r$-direction, while the third quadrant corresponds to a trapped region, where they propagate in the negative $r$-direction. For $v_q$ in (5), thus, we choose the plus sign when $\{h/q, 2h/(2q-1)\} > \lambda_0/2$ and the minus sign when $\{h/q, 2h/(2q-1)\} \leqslant \lambda_0/2$, where $\lambda_0\ (= c/f_1)$ is the resonant wavelength.

Thus, when $\{h, 2h\} > \lambda_0/2$, at least one of the roots $v_q$ is in the first quadrant; the resonant mode is in the leaky state, where a part of energy leaks away from the resonator in the radial direction [7]. On the other hand, when $\{h, 2h\} \leqslant \lambda_0/2$, $v_q$ for any $q$ value is always in the third quadrant; the resonant mode is in the trapped state, where the energy is trapped in and near the rod without radiation [7]. Particularly, the case of $\{h, 2h\} = \lambda_0/2$ represents a cutoff of the trapped state.

### B. Analysis by Perturbation Technique

The technique due to the perturbation theory described here allows us to separately estimate the $Q_c$ and $Q_d$ values from only the computation of resonant frequencies for structures without radiation. Then consider the real numbers for all variables in (1)–(7), such as $\omega$ and $\epsilon_r$. For the parallel-plates-type resonators in Fig. 1(a) and (b), the $TE_0$ mode is in the trapped state when $\{h, 2h\} \leqslant \lambda_0/2$, as described above. In this case, the term containing the Hankel functions in (2) is modified as follows:

$$\frac{H_1(v_q)}{v_q H_0(v_q)} \to -\frac{K_1(v_q')}{v_q' K_0(v_q')} \quad v_q' = \sqrt{\left(\frac{R}{L} Z_q\right)^2 - \left(\frac{\omega R}{c}\right)^2} \tag{12}$$

since $v_q = -jv_q'$ for any $q$ value, where $K_n(x)$ is the modified Bessel function of the second kind. Furthermore, for the cavity-open-type resonator in Fig. 1(c), the following exchange in (2) is needed [7]:

$$\frac{H_1(v_q)}{v_q H_0(v_q)} \to \frac{I_1(v_q')K_1(v_q'S) - I_1(v_q'S)K_1(v_q')}{v_q'\left[I_0(v_q')K_1(v_q'S) + I_1(v_q'S)K_0(v_q')\right]} \tag{13}$$

where $S = a/R = d/D$ and $I_n(x)$ is the modified Bessel function of the first kind.

Following Kajfez's method, we can compute the $Q_c$ values from

$$\frac{1}{Q_c}=\frac{1}{Q_{cu}}+\frac{1}{Q_{cl}}$$
$$\frac{1}{Q_c}=\frac{2}{Q_{cu}}$$
$$\frac{1}{Q_c}=\frac{2}{Q_{cu}}+\frac{1}{Q_{cy}} \tag{14}$$

for Fig. 1(a), (b), and (c), respectively, where

$$Q_{cu}=\frac{f_0}{(-\Delta f_0/\Delta M)\delta_c}$$
$$Q_{cl}=\frac{f_0}{(-\Delta f_0/\Delta L)\delta_c}$$
$$Q_{cy}=\frac{f_0}{(-\Delta f_0/\Delta d)2\delta_c} \tag{15}$$

and $Q_{cu}$, $Q_{cl}$, and $Q_{cy}$ are ones due to the conductor losses of the upper and lower plates and of the cylinder, respectively. The resonant frequency $f_0$ and the frequency shift $\Delta f_0$ due to the cavity-wall perturbation, such as $\Delta M$, $\Delta L$, or $\Delta d$, can accurately be computed from (1). Also, $\delta_c=(\pi f_0\mu\sigma)^{-1/2}$ is the skin depth of the conductor, where $\mu$ is its permeability and $\sigma$ is its conductivity.

In the following, we derive a formula for $Q_d$ from the cavity-material perturbation. Consider a cavity filled partially with dielectric. From the definition of $Q_d$, at first, we obtain

$$Q_d=\omega\frac{W}{P_d}=\frac{1}{\tan\delta}\frac{W_d+W_a}{W_d} \tag{16}$$

since $W=2(W_d+W_a)$ and $P_d=2\omega W_d\tan\delta$, where $W_d$ and $W_a$ are the electric energy stored in the dielectric and in the air, respectively, and $P_d$ is the average power dissipated in the dielectric. Then, applying a formula for cavity-material perturbations [9] to this cavity, we obtain

$$\frac{\Delta f_0}{f_0}=-\frac{\Delta\epsilon_r}{2\epsilon_r}\frac{W_d}{W_d+W_a} \tag{17}$$

from the frequency shift $\Delta f_0$ due to the dielectric perturbation $\Delta\epsilon_r$ only. Hence, substituting (17) into (16) yields the following formula for $Q_d$:

$$Q_d=\frac{1}{\tan\delta}\frac{f_0}{(-\Delta f_0/\Delta\epsilon_r)2\epsilon_r} \tag{18}$$

where the value of $-\Delta f_0/\Delta\epsilon_r$ also can be computed accurately from (1). Note that (18) is valid for all modes including the hybrid modes. With (14) and (18), thus, the unloaded $Q$, $Q_u$, is given by

$$\frac{1}{Q_u}=\frac{1}{Q_c}+\frac{1}{Q_d} \tag{19}$$

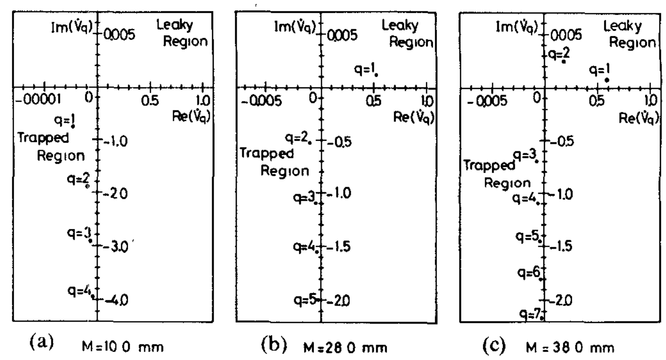


Fig. 2. Locations of $v_q$ for the parallel-plates-image-type resonator in Fig. 3, as $M$ is varied.

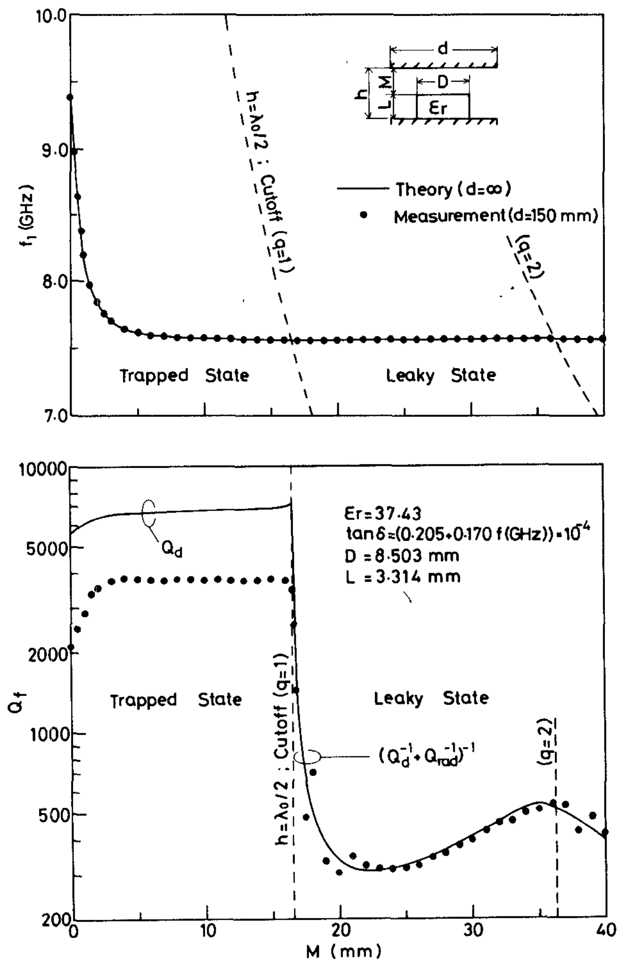


Fig. 3. Computed results of complex frequencies $(f_1, Q_f)$ and measured results $(f_0, Q_u)$ for the $TE_{01(1+\delta)/2}$ mode of the parallel-plates-image-type resonator.

## III. Computations and Experiments for Parallel-Plates-Type Resonators

To verify the validity of these theories, we performed the computations and experiments for the parallel-plates-type resonators, using a $(Zr\cdot Sn)TiO_4$ ceramic rod with $\epsilon_r=37.43$ and $\tan\delta=(0.205+0.170f_0[\mathrm{GHz}])\times10^{-4}$ (Murata Mfg. Co., Ltd.) and two copper plates with the relative conductivity of $\bar{\sigma}=\sigma/\sigma_0=0.92$, where $\sigma_0=58\times10^6$ S/m is the conductivity of the international standard annealed copper.

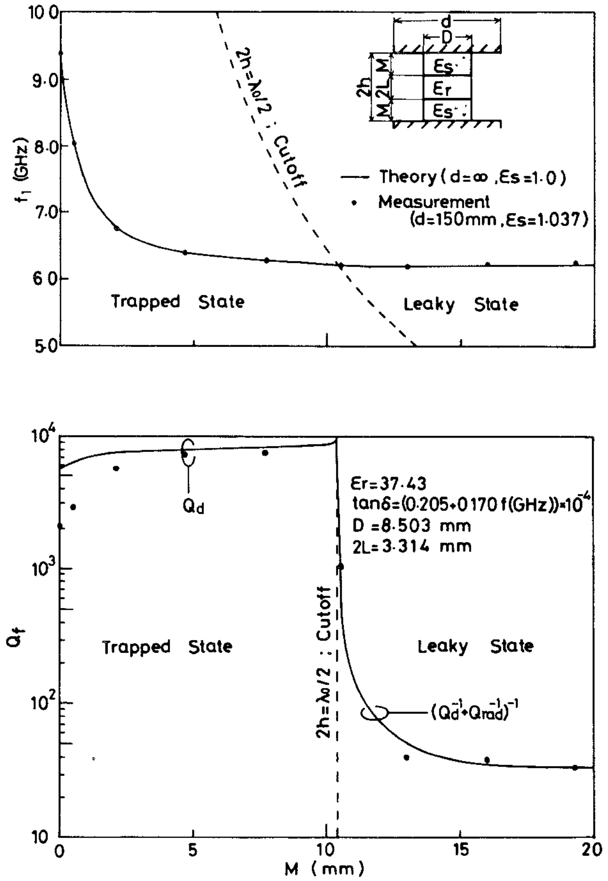


Fig. 4. Computed results of complex frequencies $(f_1, Q_f)$ and measured results $(f_0, Q_u)$ for the $TE_{01\delta}$ mode of the parallel-plates-open-type resonator.

These values were measured by a dielectric rod resonator method [10].

At first, the complex frequencies versus the distance $M$ were computed for the $TE_{01\ (1+\delta)/2}$ mode of the parallel-plates-image-type resonator in Fig. 1(a). Fig. 2 shows the locations of $v_q$ in the complex $v$ plane. At $M = 10$ mm, all $v_q$ values lie in the third quadrant (Fig. 2(a)). As $M$ increases and $h$ becomes greater than $\lambda_0/2$, only $v_1$ moves into the first quadrant (Fig. 2(b)). The number of $v_q$'s in this quadrant increases with $M$ (Fig. 2(c)). The computed results are shown in Fig. 3 by solid lines. Similar results for the $TE_{01\delta}$ mode of the parallel-plate-open-type resonator are also shown in Fig. 4. Broken lines in both figures show the cutoffs. The left-hand side of the cutoff is the trapped state region while the right-hand side is the leaky state region. When $M$ passes through the cutoff, the $Q_f$ values rapidly decrease owing to the radiation loss. In Fig. 3, particularly, a gentle peak of $Q_f$ appears near the transition of $v_2$ from the trapped to leaky region. Also, Fig. 5 shows the convergence of the solutions for these resonators versus the number $N$ of the determinant. The solutions to three significant figures can be obtained when $N \simeq 15$ for Fig. 5(a) and $N \simeq 7$ for Fig. 5(b).

The dots in Figs. 3 and 4 indicate the measured values. An experimental procedure taken is similar to that described in [10]. In both cases, the theoretical $f_1$ curves

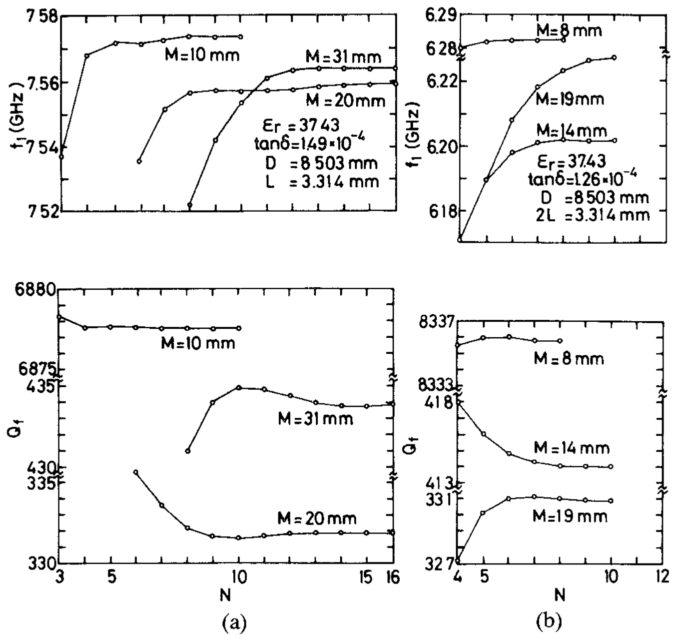


Fig. 5. Convergence of complex frequencies $(f_1, Q_f)$ for (a) the parallel-plates-image-type resonators in Fig. 3 and for (b) the parallel-plates-open-type resonator in Fig. 4.

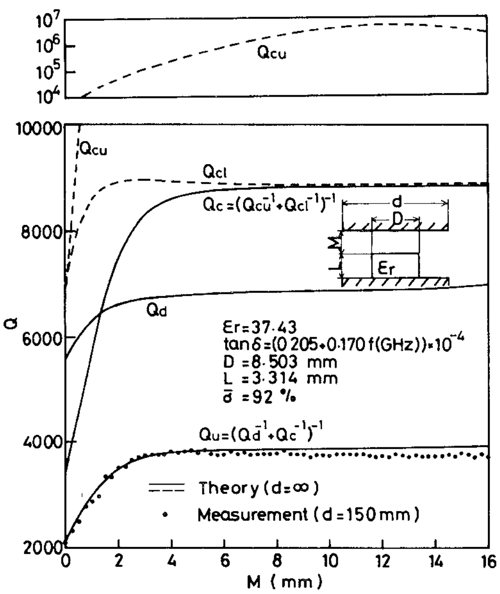


Fig. 6. Computed $Q$ values due to the perturbation theory and measured $Q_u$ values for the trapped state $TE_{01\ (1+\delta)/2}$ mode of the parallel-plates-image-type resonator.

agree very well with the measured $f_0$ values. The theoretical $Q_f$ curves in the trapped state, which actually means $Q_d$, are greater than the measured $Q_u$ values because the conductor is supposed to be lossless in this analysis. On the other hand, the $Q_f$ curves in the leaky state, which consist of $Q_d$ and $Q_{\rm rad}$, agree well with the measured $Q_u$ values because the radiation loss is predominant.

For the same structures as used above, then, the $Q_c$, $Q_d$, and $Q_u$ values in the trapped state were computed using the perturbation technique, that is, from (14), (18), and (19). The respective results are shown in Figs. 6 and 7,

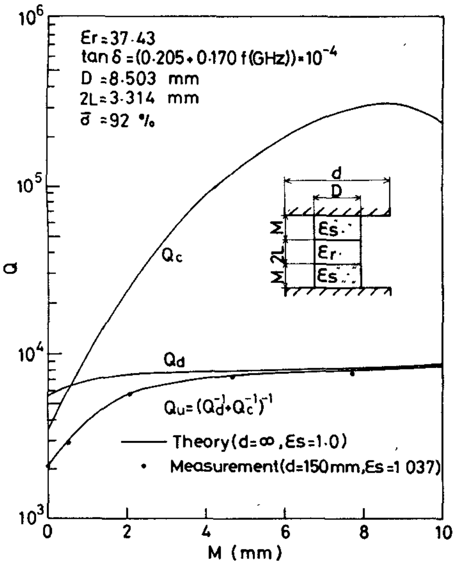


Fig. 7. Computed $Q$ values due to the perturbation theory and measured $Q_u$ values for the trapped state $TE_{01\delta}$ mode of the parallel-plates-open-type resonator.

where the computed $f_0$ curves are omitted since they are identical with the $f_1$ curves given in Figs. 3 and 4. The $Q_d$ values computed from (18) agree to within 0.05 percent with the computed $Q_f$ values in the trapped states in Figs. 3 and 4. The $Q_c$ values increase rapidly with increasing $M$. Also, the computed $Q_u$ curves agree well with the measured $Q_u$ values which are reproductions of those in Figs. 3 and 4. Thus, validity of these two techniques was verified.

## IV. Possibility of High-$Q$ Dielectric Resonators

Finally, for the $TE_{01\delta}$ mode of the cavity-open-type resonator in Fig. 1(c), the computed results are shown in Fig. 8. In this computation, we used the optimum dimensions to obtain the best separation of higher order modes [8]. The $f_0$ curve was computed from (1) and the $Q$ curves were computed by means of the perturbation technique when $\bar{\sigma}=1.0$ (copper), and $\tan\delta=10^{-4}$ and $10^{-5}$. When $\epsilon_r=37.5$ and $D=10$ mm, the optimum values are $2L=4.19$ mm, $M^o=5.26$ mm, and $d=27.0$ mm, and then we get $f_0=5.37$ GHz. In this case, we obtain $Q_d\tan\delta=1.026$ and $Q_c=1.30\times10^5$ since $Q_{cu}=3.40\times10^5$ and $Q_{cy}=5.54\times10^5$. Thus, we obtain $Q_u=9520$ for $\tan\delta=10^{-4}$ and also $Q_u=57000$ for $\tan\delta=10^{-5}$. For a $TE_{011}$ empty cavity, on the other hand, the theoretical maximum $Q_u$ value, attained when $d=2h$, is 41000 at $f_0=5.4$ GHz. As a result, if low-loss materials with $\tan\delta$ of nearly $10^{-5}$ are developed, shielded dielectric resonators will realize the $Q_u$ values higher than those of conductor cavities.

## V. Conclusion

It is concluded that the two approaches presented are effective for the separate, accurate estimation of $Q$-factors due to the radiation, conductor, and dielectric losses for the circularly-symmetric $TE_0$ modes of the shielded dielectric resonators. The computed results show that the $Q$-value due to the conductor loss increases rapidly as the conductor is moved away from the dielectric. As a result, a possibility of realizing high-$Q$ dielectric resonators in the microwave region was suggested. In addition, a practical application for such resonators in the millimeter-wave region also can be expected as suggested by Dydyk [11].

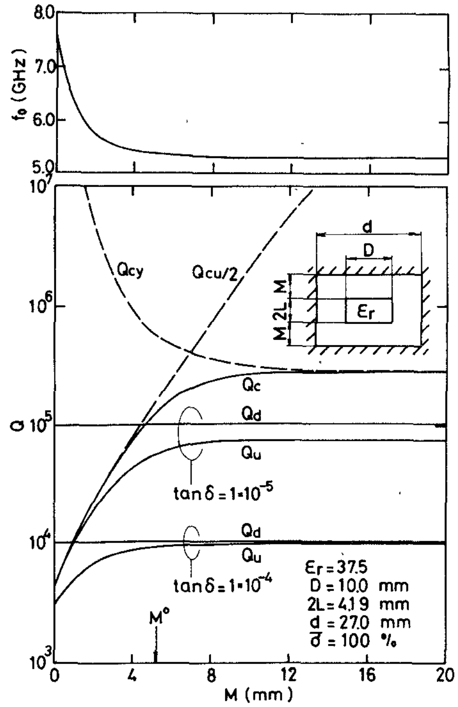


Fig. 8. Computed $Q$ values due to the perturbation theory for the $TE_{01\delta}$ mode of the cavity-open-type resonator.

## References

[1] J. Delaballe, P. Guillon, and Y. Garault, "Local complex permittivity measurement of MIC substrates," *Arch. Elek. Übertragung.*, vol. 35, pp. 80–83, Feb. 1981.
[2] M. Dydyk, "Dielectric resonators add $Q$ to MIC filters," *Microwaves*, vol. 16, pp. 150–160, Dec. 1977.
[3] R. D. Smedt, "Dielectric resonator inside a circular waveguide," *Arch. Elek. Übertragung.*, vol. 38, pp. 113–120, Mar./Apr. 1984.
[4] Y. Kobayashi and S. Tanaka, "Resonant modes of a dielectric rod resonator short-circuited at both ends by parallel conducting plates," *IEEE Trans. Microwave Theory Tech.*, vol. MTT-28, pp. 1077–1085, Oct. 1980.
[5] S. Maj and J. W. Modelski, "Application of a dielectric resonator on microstrip line for a measurement of complex permittivity," in *1984 IEEE MTT-S Int. Microwave Symp. Dig.*, no. 23-6, pp. 525-527.
[6] D. Kajfez, "Incremental frequency rule for computing the Q-factor of a shielded $TE_{0mp}$ dielectric resonator," *IEEE Trans. Microwave Theory Tech.*, vol. MTT-32, pp. 941–943, Aug. 1984.
[7] Y. Kobayashi, N. Fukuoka, and S. Yoshida, "Resonant modes for a shielded dielectric rod resonator," *Trans. IECE Japan*, vol. J64-B, pp. 433-440, May 1981. (translated in English, *Electronics and Communications in Japan*, vol. 64-B, pp. 44–51, Nov. 1981.)
[8] Y. Kobayashi and M. Miura, "Optimum design of shielded dielectric rod and ring resonators for obtaining the best mode separation," in *1984 IEEE MTT-S Int. Microwave Symp. Dig.*, no. 7-11, pp. 184–186.
[9] R. F. Harrington, *Time-Harmonic Electromagnetic Fields.* New York: McGraw-Hill, 1961, pp. 321–326.

[10] Y. Kobayashi and M. Katoh, "Microwave measurement of dielectric properties of low-loss materials by dielectric rod resonator method," *IEEE Trans. Microwave Theory Tech.*, vol. MTT-33, pp. 586–592, July 1985.
[11] M. Dydyk, "Apply high-$Q$ resonators to mm-wave microstrip," *Microwaves*, vol. 19, pp. 62–63, Dec. 1980.

**Yoshio Kobayashi** (M'74) was born in Gumma, Japan, on July 4, 1939. He received the B.E., M.E., and D. Eng. degrees in electrical engineering from Tokyo Metropolitan University, Tokyo, Japan, in 1963, 1965, and 1982, respectively.

He was a Research Assistant from 1965 to 1968, and a Lecturer from 1968 to 1982 in the Department of Electrical Engineering, Saitama University, Urawa, Saitama, Japan. He is now an Associate Professor at the same University. His current research interests are in dielectric waveguides and resonators, dielectric resonator filters, and measurement of dielectric materials, in the microwave and millimeter-wave region.

Dr. Kobayashi is a member of the Institute of Electronics and Communication Engineers of Japan, and the Institute of Electrical Engineers of Japan.

**Takayuki Aoki** was born in Saitama, Japan, on April 20, 1959. He received the B.E. and M.E. degrees in electrical engineering from Saitama University, Saitama, Japan, in 1982 and 1984, respectively.

In 1984, he joined the Transmission Division, NEC Corporation, Kawasaki, Japan.

Mr. Aoki is a member of the Institute of Electronics and Communication Engineers of Japan.

**Yukimasa Kabe** was born in Gumma, Japan, on November 30, 1962. He received the B.E. degree in electrical engineering from Saitama University, Saitama, Japan in 1985. Currently, he is studying toward the M.E. degree at Saitama University. His research activities have been concerned with microwave and millimeter-wave applications of dielectric resonators.

Mr. Kabe is a associate member of the Institute of Electronics and Communication Engineers of Japan.